A least-squares collocation approach to integrate InSAR and GNSS observations: CoInSAR

Chong-You Wang [1] Demián Gómez [1] Mara Figueroa [1 2]

[1]Division of Geodetic Science, School of Earth Sciences, The Ohio State University, USA
[2]Solid Earth and Ice Group, Jet Propulsion Laboratory, California Institute of Technology, Pasadena, CA, USA.

Introduction

Surface displacements measured by InSAR are commonly integrated with ground-based Global Navigation Satellite System (GNSS) measurements. The integration process requires accounting for **reference frame discrepancies** and **measurement uncertainties**. However, the common integration methods usually ignore GNSS and InSAR measurement errors. In addition, the integration is generally achieved in velocity field, which restricts the application to linear deformations. In this study, we propose CoInSAR, an approach **using least-squares collocation (LSC)** (Moritz, 1978) to **transform InSAR displacement time series into the GNSS reference frame while correcting turbulent tropospheric errors**. We account for the **random noise in both displacement measurements and the turbulent tropospheric delays** which typically persist in InSAR data after the correction of systematic errors. With LSC, our method yields an **unbiased solution for the reference frame transformation parameter, interpolates corrections for turbulent tropospheric errors and produces integrated displacement time series**.

Observation and Stochastic Models

Prior to applying CoInSAR, deterministic error sources need to be corrected from both GNSS and InSAR measurements, leaving the remaining errors behaving stochastically. Regarding InSAR, the error sources are categorized as:

Deterministic:

- Topography-dependent and large-scale tropospheric delays (required)
- DEM errors (required)
- Ionospheric delays (not always corrected)
- Orbital errors (not always corrected)

Stochastic:

- Decoherence-related errors
- Turbulent tropospheric delays

Note that we assume turbulent tropospheric delays still persist after tropospheric correction because the current correction approaches typically only remove the deterministic component of tropospheric delays.

We first project GNSS three-dimensional daily solutions from continuous GNSS stations into the LOS direction and obtain InSAR measurements at GNSS stations. For GNSS data gaps at some epochs, we predict them using the Extended Trajectory Model (Bevis & Brown, 2014). Then, we formulate the observation and stochastic models at each SAR epoch k as:

$$\mathbf{d}_k = \mathbf{A}x_k + \mathbf{e}_k^{GNSS} + \mathbf{e}_k^{InSAR} + \mathbf{s}_k \tag{1}$$

$$\mathbf{e}_k^{GNSS} \sim (0, \mathbf{C}_{ee}^{GNSS}),\ \ \mathbf{e}_k^{InSAR} \sim (0, \mathbf{C}_{ee}^{InSAR}),\ \ \mathbf{s}_k \sim (0, \mathbf{C}_{ss}) \tag{2}$$

where $\mathbf{d}_k$ is the vector of difference between GNSS and InSAR displacements, A is the design matrix, x_k is the reference frame transformation parameter between two data (one translation). $\mathbf{e}_k^{GNSS}$, $\mathbf{e}_k^{InSAR}$ and $\mathbf{s}_k$ are the vectors of GNSS random noise, InSAR random noise, and turbulent tropospheric error correction, respectively, with corresponding covariance matrices $\mathbf{C}_{ee}^{GNSS}$, $\mathbf{C}_{ee}^{InSAR}$ and $\mathbf{C}_{ss}$.

We construct $\mathbf{C}_{ee}^{GNSS}$ based on posteriori variance of daily solutions or variance of the ETM-predicted displacements. $\mathbf{C}_{ee}^{InSAR}$ is derived from interferometric coherence (Rodriguez & Martin, 1992): convert to interferometric phase variance, propagate to phase variance of time series and convert to range variance.

We build $\mathbf{C}_{ss}$ directly from InSAR displacements by:

1. **Temporally**, removing deformation signals using ETM that accounts for linear deformations, seasonal variations, earthquakes (optional), and postseismic transients (optional)
2. **Spatially**, removing unmodeled spatial long-wavelength signals with second-order polynomial surface
3. Computing the empirical covariance using the detrended spatial residual field at epoch k:

$$\mathbf{C}_k(d) = \frac{1}{N_d}\sum_{i,j}^{N_d} r_{k,i} r_{k,j}, \tag{3}$$

where $r_{k,i}$ and $r_{k,j}$ are the detrended residuals at two locations separated by a distance d, and N_d is the number of residual pairs.

4. Fitting Cauchy covariance function to the empirical covariance:

$$f(d) = \frac{a_0}{1 + (\frac{d}{a_1})^2} \tag{4}$$

5. Using the covariance function to construct $\mathbf{C}_{ss}$

Integration

We aim to estimate the transformation parameter x_k and interpolate the correction of turbulent tropospheric delays for all InSAR measurement locations at epoch k. x_k is estimated using a weighted least-squares approach:

$$x_k = (\mathbf{A}^T(\mathbf{C}_{ss} + \mathbf{C}_{ee}^{GNSS} + \mathbf{C}_{ee}^{InSAR})^{-1}\mathbf{A})^{-1}\mathbf{A}^T(\mathbf{C}_{ss} + \mathbf{C}_{ee}^{GNSS} + \mathbf{C}_{ee}^{InSAR})^{-1}\mathbf{d}_k \tag{5}$$

Then, we obtain the residual $\mathbf{v_k}$ and use it to interpolate the correction of turbulent tropospheric delays at all InSAR measurement locations, $\mathbf{z}$:

$$\mathbf{v}_k = \mathbf{d}_k - \mathbf{A}x_k \tag{6}$$

$$\mathbf{z} = \mathbf{G}\mathbf{v}_k \tag{7}$$

Based on the principle of Best Linear Unbiased Predictor, $\mathbf{G}$ is obtained as:

$$Var(\mathbf{z} - \mathbf{G}\mathbf{v}_k) = \min,\ \ E(\mathbf{z}) = E(\mathbf{G}\mathbf{v}_k), \tag{8}$$

$$\mathbf{G} = \mathbf{C}_{zs}(\mathbf{C}_{ss} + \mathbf{C}_{ee}^{GNSS} + \mathbf{C}_{ee}^{InSAR})^{-1}, \tag{9}$$

where $\mathbf{C}_{zs}$ is the cross-covariance matrix of turbulent tropospheric delays between interpolation positions and GNSS station locations. Substituting Eq. 9 into Eq. 7, we obtain $\mathbf{z}$ as:

$$\mathbf{z} = \mathbf{C}_{zs}(\mathbf{C}_{ss} + \mathbf{C}_{ee}^{GNSS} + \mathbf{C}_{ee}^{InSAR})^{-1}(d_k - \mathbf{A}x_k) \tag{10}$$

Finally, the integration is achieved by applying x_k and $\mathbf{z}$ to all InSAR displacements $\mathbf{d_k^{InSAR}}$:

$$\mathbf{d_k^{merge}} = \mathbf{d_k^{InSAR}} + \bar{\mathbf{A}}x_k + \mathbf{z} \tag{11}$$

Application

Dataset

- GNSS: Daily solutions from Nevada Geodetic Laboratory. Solid earth tide (SET) and ocean tide loadings (OTL) are removed.
- InSAR: Sentinel-1 time series from LiCSAR and LiCSBAS (Lazecký et al., 2020; Morishita et al., 2020). Corrected for tropospheric delay (GACOS), DEM errors, SET and OTL.

Land Subsidence in San Joaquin Valley, USA

We used 261 ascending interferograms in 2020 and 56 continuous GNSS stations. InSAR data with elevations below 500 meters and temporal coherence above 0.3 were selected.

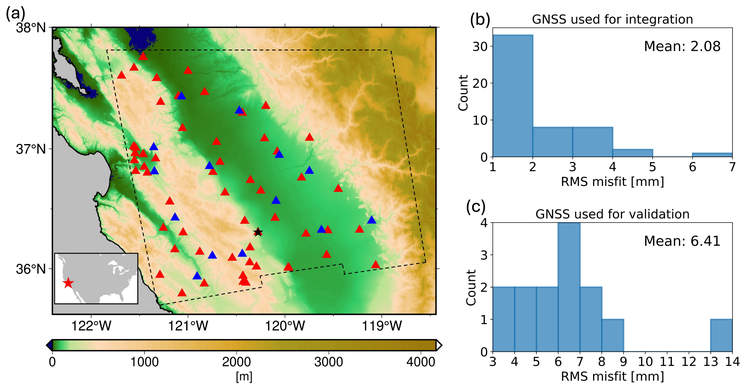

Figure 1. (a) Study area in San Joaquin Valley. Black dashed line delimits the cropped SAR frame. Black star is the reference area for InSAR displacements. Red and blue triangles show GNSS stations used for integration and validation, respectively. (b) and (c) Histograms of RMS misfit between CoInSAR and GNSS time series.

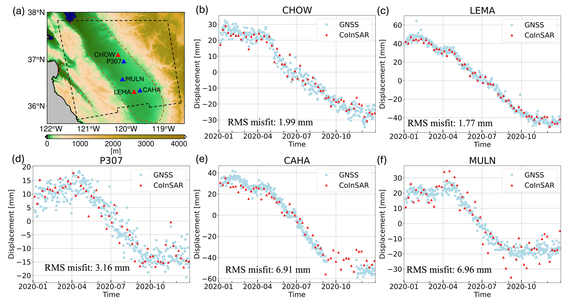

Figure 2. Comparison between CoInSAR and GNSS time series. (a) location map showing two GNSS stations used for integration in CoInSAR (red triangles) and three GNSS stations used for validation (blue triangles). (b) and (c) time series at GNSS stations used for integration, and (d)-(f) time series at GNSS stations used for validation. RMS misfits calculated with respect to GNSS time series.

Seismic deformations in Coquimbo region, Chile

We used 829 descending interferograms from Oct. 2014 to July 2022 and 10 continuous GNSS stations. InSAR data with temporal coherence above 0.5 are used for the integration.

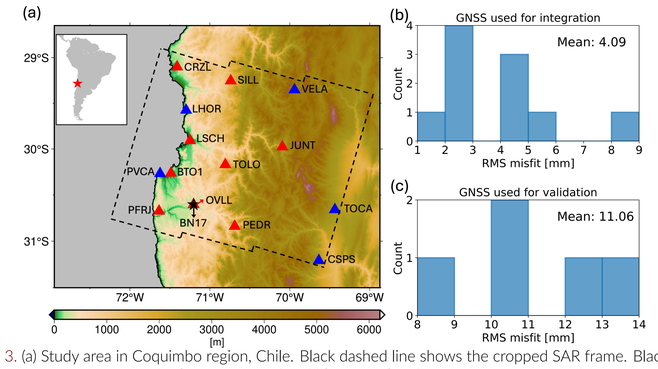

Figure 3. (a) Study area in Coquimbo region, Chile. Black dashed line shows the cropped SAR frame. Black star is the reference area for InSAR displacements. Red and blue triangles show GNSS stations used for integration and validation, respectively. (b) and (c) Histograms of RMS misfit between CoInSAR and GNSS time series.

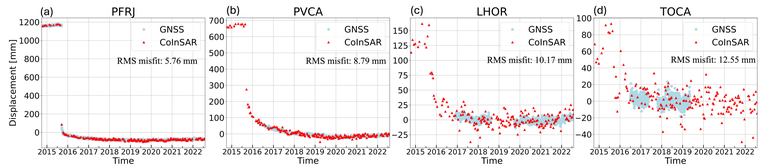

Figure 4. Comparison between CoInSAR and GNSS time series. (a) time series at GNSS stations used for integration. (b)-(d) time series at GNSS stations used for validation. RMS misfits calculated with respect to GNSS time series.

Co- and Postseismic deformations of the Illapel earthquake

We used the CoInSAR time series and ETM to estimate the co- and postseismic deformations associated with the Illapel earthquake on Sep. 16, 2015. Three-frame SAR interferograms were used from late 2014 through the most recent acquisition date. We selected 1500 InSAR pixels with temporal coherence above 0.7 for the comparison between the derived coseismic and 50-day postseismic deformations and the geophysical model from Figueroa et al. (2024).

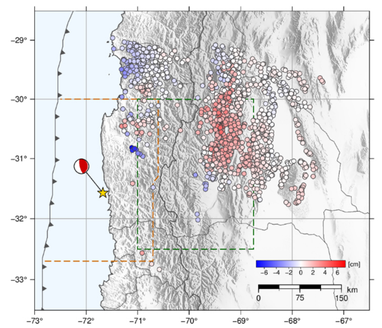

Figure 5. Residual between Co- and postseismic deformations and the model by Figueroa et al. (2024).

Conclusion

Our integration method has four strengths:

- We estimate the stochastic model of turbulent tropospheric delays based on InSAR data.
- We account for random noise from both data and turbulent tropospheric delays through their stochastic models to estimate the reference frame transformation parameter.
- We mitigate turbulent tropospheric delays by stochastic interpolation.
- Our method enables time-series integration, which makes it applicable to linear and non-linear deformations, as validated by the case studies.

References

Bevis, M., & Brown, A. (2014). Trajectory models and reference frames for crustal motion geodesy. *Journal of Geodesy*, *88*(3), 283–311. https://doi.org/10.1007/s00190-013-0685-5

Figueroa, M., Sobrero, F., Gómez, D., Smalley Jr, R., Bevis, M., Griffith, W., Caccamise, D., & Kendrick, E. (2024). Creep on the argentine precordillera décollement following the 2015 illapel, chile, earthquake: Implications for andean seismotectonics. *Geophysical Research Letters*, *51*(19), e2024GL110945.

Lazecký, M., Spaans, K., González, P. J., Maghsoudi, Y., Morishita, Y., Albino, F., Elliott, J., Greenall, N., Hatton, E., Hooper, A., et al. (2020). Licsar: An automatic insar tool for measuring and monitoring tectonic and volcanic activity. *Remote Sensing*, *12*(15), 2430.

Morishita, Y., Lazecky, M., Wright, T. J., Weiss, J. R., Elliott, J. R., & Hooper, A. (2020). Licsbas: An open-source insar time series analysis package integrated with the licsar automated sentinel-1 insar processor. *Remote Sensing*, *12*(3), 424.

Moritz, H. (1978). Least-squares collocation. *Reviews of geophysics*, *16*(3), 421–430.

Rodriguez, E., & Martin, J. (1992). Theory and design of interferometric synthetic aperture radars. *IEE proceedings f (radar and signal processing)*, *139*(2), 147–159.